Smart Structures and Systems, *Vol. 26, No. 5 (2020) 667-680*
DOI: https://doi.org/10.12989/sss.2020.26.5.667

Performance assessment of bridges using short-period structural health monitoring system: Sungsu bridge case study

Mosbeh R. Kaloop[1,2,3a], Mohamed Elsharawy[4b], Basem Abdelwahed[5c], Jong Wan Hu[1,2d] and Dongwook Kim[*1]

[1]*Department of Civil and Environmental Engineering, Incheon National University, Korea*
[2]*Incheon Disaster Prevention Research Center, Incheon National University, Incheon, Korea*
[3]*Public Works and Civil Engineering Department, College of Engineering, Mansoura University, Egypt*
[4]*Civil and Construction Engineering Department, College of Engineering, Imam Abdulrahman Bin Faisal University, Saudi Arabia*
[5]*Structural Engineering Department, College of Engineering, Mansoura University, Egypt*

(*Received April 5, 2020, Revised July 4, 2020, Accepted July 6, 2020*)

Abstract. This study aims at reporting a systematic procedure for evaluating the static and dynamic structural performance of steel bridges based on a short-period structural health monitoring measurement. Sungsu bridge located in Korea is considered as a case study presenting the most recent tests carried out to examine the bridge condition. Short-period measurements of Structural Health Monitoring (SHM) system were used during the bridge testing phase. A novel symmetry index is introduced using statistical analyses of deflection and strain measurements. Frequency Domain Decomposition (FDD) is implemented to the strain measurements to estimate the bridge mode shapes and damping ratios. Furthermore, Markov Chain Monte Carlo (MCMC) is also implemented to examine the reliability of bridge performance while ambient design trucks are in static or moving at different speeds. Strain, displacement and acceleration were measured at selected locations on the bridge. The results show that the symmetry index can be an efficient and useful measure in assessing the steel bridge performance. The results from the used method reveal that the performance of the Sungsu bridge is safe under operational conditions.

Keywords: bridge; output-only; behavior; frequency domain decomposition complex

1. Introduction

The development of a country depends significantly on the service-conditions of its infrastructure projects. Bridges are one of the main components of any transportation infrastructure network. The number of bridges constructed worldwide has been significantly increased in the last few decades. However, some of these bridges were designed according past design codes and standards or have already passed over 30 years in service. Moreover, deterioration impacts may occur due to natural disasters, the increase in traffic volumes, weather conditions and/or material strength degradation (i.e., corrosion, soil scour and others), which may have significant reduction on its structural capacity or may urgently require action. A collapse or closure of bridges can lead to traffic chaos in regions, significant financial losses, and, in some cases, heavy casualties. Many cases of bridge collapse occurred in the USA, Japan, Korea, Italy and elsewhere have brought the attention to the importance of continuous monitoring and carrying out the required periodic inspection for such highly important structures; 2000 till now, over 100 bridges have been damaged due to different cases of loads (https://en.wikipedia.org/wiki/List_of_bridge_failures). For instance, I-35 bridge, arch/truss bridge, over the Mississippi river, had been damaged in 2007 due to overloading. Truss bridge, Eggner Ferry bridge, in the USA, in 2012 had been damaged also due to ship collision. Dale Bend truss bridge in the USA had been damaged in 2019 due to heavy truck overload passed over the bridge. In addition, 43 people were dead in 2018 due to Ponte Morandi bridge collapse in Italy. In 1991, 15 were killed during construction a bridge in Japan. In 2007, 5 workers had been killed because of a collapse during constructing a bridge in Korea, and in 1994, 32 people had been dead due to a collapse in Sungsu bridge. The structural analysis of Sungsu bridge presented that the collapse could occur due to low stiffness of a girder under overload effect (Chang *et al*. 2009).

Thus, it is important to thoroughly assess periodically the safety, serviceability and sustainability of bridges during their service life, and hence Structural Health Monitoring (SHM) systems are being actively developed to fulfill the task. SHM is considered as a key solution to provide information about the operational performance of the structures under examination. SHM is almost implemented by active and/or passive methods; the passive is an examining method used in static, dynamic and rotating equipment, whereas the active is a direct health assessment method for evaluating the structures' behavior using health

*Corresponding author, Associate Professor, E-mail: dwkim@inu.ac.kr
[a] Associate Professor, E-mail: mosbeh@mans.edu.eg
[b] Assistant Professor, E-mail: mrelsharawy@iau.edu.sa
[c] Assistant Professor, E-mail: bs_hadi@mans.edu.eg
[d] Associate Professor, E-mail: jongp24@inu.ac.kr

ISSN: 1738-1584 (Print), 1738-1991 (Online)

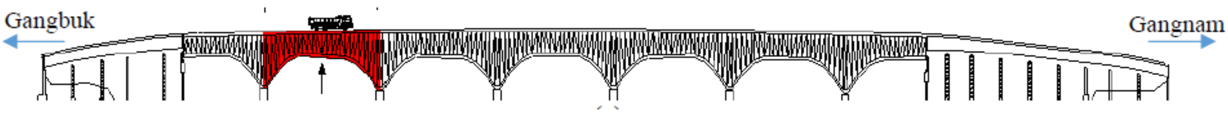

(a)

(b)

(c)

Fig. 1 Sungsu bridge (a) elevation view; (b) overall view; (c) collapse

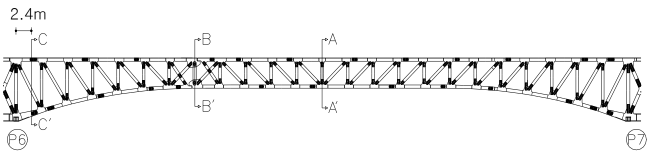

(a)

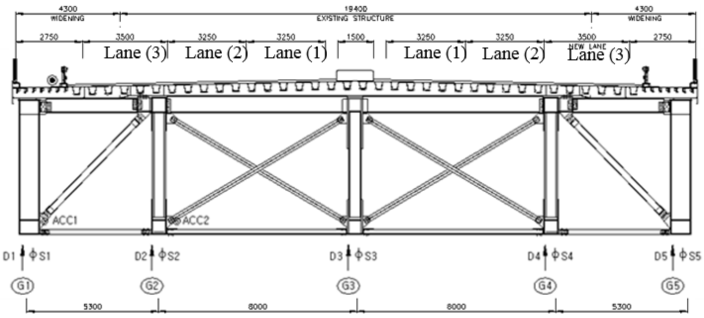

(b)

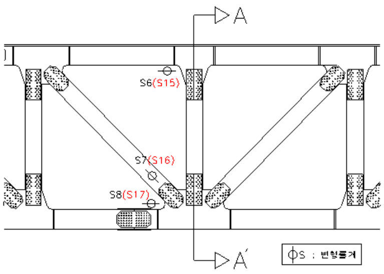

(c)

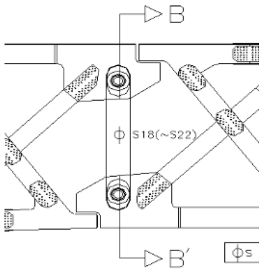

(d)

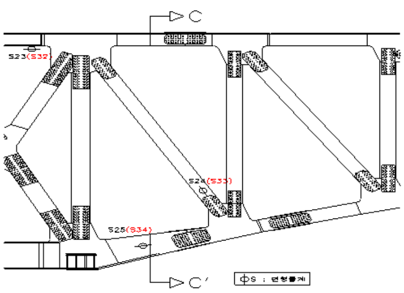

(e)

Fig. 2 SHM system of the bridge: (a) test span and monitoring sections; (b) cross section of section A-A; (b) and (c) monitoring system of section A-A; (d) and (e) monitoring system of sections B-B and C-C, respectively

detection monitoring sensors (Abbas and Mahmood 2018).

Some structures may be subjected to high vibrations and/or fatigue effects such as long-span bridges and super tall buildings. Thus, these structures essentially require detailed monitoring using Continuous Structural Health Monitoring System (CSHMS). This is obviously to capture

Table 1 Distribution of SHM sensors

Sensor	Section	Number	Girder				
			G1	G2	G3	G4	G5
Strain gauge	A-A	17	$S_{1,6,7,8}$	$S_{2,9,10}$	$S_{3,11,12}$	$S_{4,13,14}$	$S_{5,15,16,17}$
	B-B	5	S_{18}	S_{19}	S_{20}	S_{21}	S_{22}
	C-C	12	$S_{23,24,25}$	$S_{26,27}$	$S_{28,29}$	$S_{30,31}$	$S_{32,33,34}$
Displacement	A-A	5	D_1	D_2	D_3	D_4	D_5
Accelerometer	A-A	2	ACC_1	ACC_2	--	--	--
Total		41	10	8	7	7	9

any long or sudden changes in their performance or conditions. Some other structures which can be considered as rigid- or semi-rigid structures may be beneficial to be monitored using Short-period Structural Health Monitoring System (SSHMS) along with periodic testing/assessment to stand on the bridge operational state.

In general, there are two types of SHM systems, destructive and nondestructive tests, that can be used in assessing the structure performance under different loading conditions. In SSHMS, Nondestructive Testing (NDT) is dominantly used effectively to collect the measurements using high advanced monitoring sensors. NDT techniques, which are effective techniques for SHM of bridges and detecting damages, can be categorized into two major approaches: Local and global (Zolghadri 2017). The first approach (local) includes the methods that are intended to provide information from a small region of structural elements such as acoustic emission technique, ultrasonic, and infrared thermography. The second approach (global) pursues the methods that provide global information about the structural condition based on the measurements from various sensors.

In Korea, many bridges were constructed in the last century to connect between regions and serve the country's economic and social development (Chang *et al.* 2009, Koh *et al.* 2009). As most of these bridges can be considered structurally rigid, NDT-SSHMSs are commonly used to evaluate structure's behavior.

Kim *et al.* (2016) and Jeong *et al.* (2018) summarized the SHM development and Korean inspection and management rules of bridges. A typical system is designed using ambient trucks for selection sections of bridge and monitored its behavior based on a designing period time (Kaloop *et al.* 2019). For example, Seo *et al.* (2013) evaluated load rating distribution of a steel bridge using short-period SHM of strain sensors. Peiris and Harik (2016) tested the behavior of a steel bridge load capacity using short-period of strain and displacement measurements. Furthermore, many reports around the world utilized a short-period monitoring system to assess bridges' behavior of load capacities; the following references represented examples of steel bridges assessments in Korea and the USA (Barker *et al.* 1999, Commander *et al.* 2008, Xiao 2016).

While, most of past studies focused on evaluation of the performance of bridges based on the theoretical models and field monitoring measurements, the current study focuses on the evaluation using only collected output of an NDT-short-period SHM system. Sungsu bridge is considered here as a case study. The collected measurements of strain, displacement and acceleration of bridge response under traffic load were used. Thus, the three response components of the bridge (strain, displacement and acceleration) were utilized to evaluate static and dynamic bridge behavior.

Statistical analysis is also used to evaluate static performance of strain and deflection measurements of the bridge. Furthermore, Frequency Domain Decomposition (FDD) is implemented to assess the mode shapes of the bridge throughout strain measurements and cross-correlation. Then, the bridge damping is estimated based on the acceleration measurements. In addition, Markov Chain Monte Carlo (MCMC) is used to examine the probability of failure of the bridge using displacement measurements. More information about the methods used in the current study can be found in Li and Cao (2016), Kaloop *et al.* (2016), Chen *at al.* (2017) and Cheynet (2019). A close mode shape to theoretical analyses of the studied building was estimated by using FDD (Brincker *et al.* 2000). The FDD method is recognized as adequate tool in estimating the mode shapes and identifying the structure damage level using ambient responses (Brincker *et al.* 2001a, Zhang *et al.* 2005, Hu *et al.* 2010). Akköse *et al.* (2017) estimated mode shapes of highway bridges using FDD when applied water trucks, and it was concluded that the truck velocity has impact on the mode shape of the considered bridges. Furthermore, FDD is used to identify a truss steel structures and long span bridge, and it is found a suitable to estimate the mode shapes of these structures (Akköse *et al.* 2017). All of the above studies used acceleration measurements in determining mode shapes of different types of structures. Additionally, Song *et al.* (2017) evaluated the cross-correlation function and numerical simulation model to determine the model parameters, and it was concluded that the cross-correlation of output measurements could accurately identify the modal frequency and modal damping ratio of the structure.

Kaloop and Hu (2016) utilized auto-correlation function of output performance of bridge to study the dynamic behavior of bridge tower, and the conclusion showed agreement between the damping that estimated by that function and the values estimated using a simulation model. On the other hand, the probabilistic functions are used widely to evaluate the reliability or failure rate of constructions (Decò and Frangopol 2011, Mccarthy 2012, Yanweerasak *et al.* 2018). Monte Carlo simulation method was used to evaluate the reliability index of structures (Sgambi *et al.* 2014, Yilmaz *et al.* 2018). Markov chain approach is the most popular stochastic deterioration modeling technique, and has been extensively used for predicting the future conditions of infrastructure facilities at the network level (Wellalage *et al.* 2014). MCMC was developed to improve Monte Carlo technique for reducing the variance in reliability analysis (Beck and Au 2002, Li and Cao 2016). Subset simulation can produce the posterior probability density function of the failure probability instead of a constant value, and it is used to reduce the correlation in conditional samples generated by MCMC

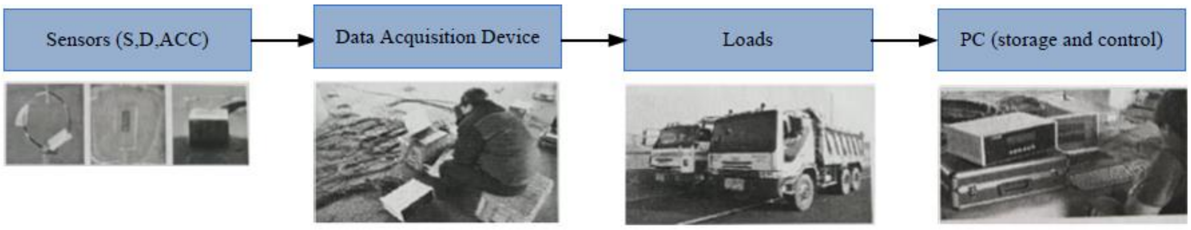

Fig. 3 SHM processing of data collection

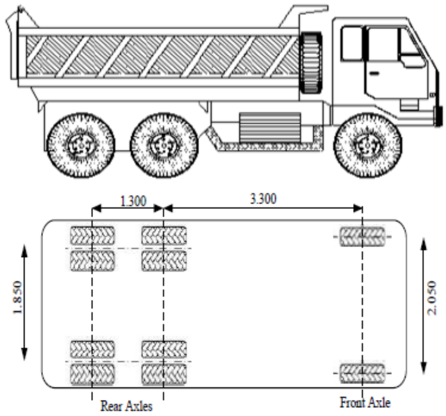

Fig. 4 Test Truck axle dimension (m)

techniques (Li and Cao 2016). In addition, the MCMC utilized subset simulation to simulate the reliability computation of structures, and standard deviation and initial sample size are the most important factor for the subset simulation (Proppe 2017). Beck and Au (2002) found the subset simulation MCMC method is able to simulate the dynamic data of structures. Further detail and method background can be found in Li and Cao (2016).

This study intended to use the output-only of the monitoring system of Sungsu bridge for evaluating its structural integrity and behavior through static and dynamic tests of ambient trucks. Symmetry behavior of the bridge is evaluated using static measurements of strain and displacement, and novel symmetry index is presented. The bridge dynamic factor is also assessed using dynamic test results. Moreover, a novel application for FDD is implemented and the strain measurements are used in the current study, to identify the mode shapes of the bridge; while, the acceleration measurements are used to estimate the damping levels of the bridge. In addition, the deflection of bridge under ambient truck is utilized to estimate the probability of failure; a design system is developed in order to estimate the reliability index of the bridge.

2. Sungsu bridge short-period measurements

Sungsu bridge crosses the Han river in Seoul, Korea connecting the two Gangbuk and Gangnam areas (Fig. 1). The total length and width of the bridge deck are 1160 m and 28 m, respectively. The dimensions of the cross section are given in Fig. 2. The bridge consists of a steel truss structures divided into simple steel, 7 spans, and concrete, 16 spans, synthetic column structures at the start and end of the bridge (Fig. 2). The length of the steel truss division is 672 m. Five spans at the middle of the steel truss division have length of 120 m. The fixing support digit of the steel truss, which issued bridge pier dry pitching of both sides, becomes the Gerber-structure that hangs and supports suspension digit of the center of the 48 m length in the vertical member.

In October 1994, the girder truss bridge, Sungsu bridge, which was originally built in 1979, collapsed 15 years after opening to the public. The collapse of this bridge (shown in Fig. 1(c)) raised enormous concerns among Korean society, and caused nationwide safety awareness towards civil structures (Chang *et al*. 2009). As a result, the Korean government started to implement construction safety related provisions in both existing and newly constructed structures, including a law that enforced safety inspection and established a new official maintenance organization. For that, a periodic monitoring system was designed for the bridge to evaluate the behavior and manage any disaster may occur in future time.

This study utilized a short-period SHM measurements had been collected on September 2, 2016 to evaluate the behavior of the bridge under designed trucks loads at the same span tested in 2011. The test was conducted for three hours (from 2 am to 5 am) to avoid the temperature effects. Similarly, to the previous tests carried out in 2011, the SHM system, including 41 sensors, was installed at three sections as presented in Fig. 2; section A-A at the midspan of suspended beam, section B-B at the expansion joint, and section C-C at truss girder. 24 sensors, as presented in Table 1, were installed at section A-A to measure deflection, vertical strain, diagonal, upper and lower chords strains, and acceleration of midspan girders. The current study evaluates the structural behavior of the truss girders (Figs. 1(a) and 2(a)). The bridge is supported by five girders, G1~G5, as shown in Fig. 2(b). Five vertical strains are supported at section B-B to check the expansion joint performance. In addition, 12 strain sensors were distributed at section C-C for measuring the truss members strain as presented in Fig. 2(e). Furthermore, the distribution of sensors on the five girders is presented in Table 1.

The sensor types used in the system are strain gauge (WFLA-6-11-1L; TML), displacement meter (CDP-50; TML) and accelerometer (ARF-10A; TML) to observe the strain (S), displacement or deflection (D) and acceleration (ACC) of the bridge girders, respectively. The monitoring system was designed to measure the movements of the girders during a short time period. Fig. 3 shows the monitoring system components used to collect the data. The

Table 2 Trucks axle's loads

Truck	Gross weight (ton)	Front wheels (ton)	Rear wheels (ton)
A	28.120	7.410	20.710
B	28.100	7.280	20.820

Table 3 Static load scenarios
[Gangbuk (A1) and Gangnam (A2)]

Load case	Direction	Lane	Trucks
LC 1	A1 → A2	3	A
LC 2	A1 → A2	2	B
LC 3	A1 → A2	2, 3	A, B
LC 4	A2 → A1	3	A
LC 5	A2 → A1	2	B
LC 6	A2 → A1	2, 3	A, B

sensors were connected to the data acquisition devices. Then, the measured data were digitized in an AD converter and delivered through the Bluetooth module and Access Point (AP). The data acquisition device used in this study have multiple channels; each device was synchronized each time by a signal sender. A personal computer was used to store the data in real time and to control the sensor nodes (data acquisition devices).

2.1 Conditional evaluation methods

The static and dynamic performances of the bridge girders were evaluated and assessed using SHM measurements.

2.1.1 Static and dynamic loads design and positions

The triaxle truck configurations used in the current test are shown on Fig. 4. Two trucks, A and B, were used in the static and dynamic tests. The weight distribution of truck along its axles are presented in Table 2. Each wheel was weighted using individual scale. The wheels were weighted three times before the test, and again three times after the test to account for any weight changes. The time histories were recorded in a calibration test using a vehicle crossing the bridge in each travel lane while regular traffic was blocked in the all directions during testing period.

Table 3 illustrates the static load cases over the three sections. Fig. 5 demonstrates the load case 3 (LC 3) of static test. Lanes 2 and 3 are used to assess the symmetry of bridge cross section, as presented in Fig. 2(b) and Table 3. The purpose of the static test is to capture the response of the bridge as a test trucks traveled across; in addition, this test is used to evaluate the response of the sensors used. In the static test, the trucks were moved by 10 km/h over bridge girder to measure the maximum response of truss members. The maximum strain and deflection were recorded and used to assess the bridge response.

Herein, static test is used to assess the symmetry performance of bridge girders. Therefore, a symmetry load cases are carried out in both sides of bridge. The symmetry performance reflects the safety serviceability of bridge behavior (Wang *et al*. 2011). Here, the displacement and strain are used to assess the symmetry of bridge girders. In this study, the linear regression is used to estimate a simple novel Symmetry Index (SI) of bridges. The slope of the regression model of both sides' performances of the bridge is used to calculate SI as follows

$$SI = |S1|/|S2| \tag{1}$$

where S1 and S2 are the slopes of the performances of bridge girders for the opposite positions of bridge cross section during static test. SI close to unity (SI = 1) refers to a high symmetry of bridge. The flowchart of the calculation of SI is presented in Fig. 6.

In dynamic load cases, the bridge was tested in one direction with having the trucks moving at different speeds. The external second lane was used to assess the girders behavior using trucks loads. Table 4 illustrates the trucks speed and directions; and Fig. 7 shows the position of trucks lane. The speed test was applied to evaluate the dynamic behavior of bridge under heavy and dynamic loads and simulate the real speeds over the bridge. Measurements were collected during different load cases, and typical measured strain, displacement, and acceleration readings for positive moment at the center span for the crawl different load test on travel lane are presented in result section.

Herein, the load dynamic factor was estimated using the collected data from the dynamic test. The strain and deflection measurements are divided into dynamic and semi-static behaviors. The semi-static behavior is extracted using low-pass filter. Therefore, the dynamic factor (DF) is calculated as follows

$$DF = \frac{R_d}{R_s} - 1 \tag{2}$$

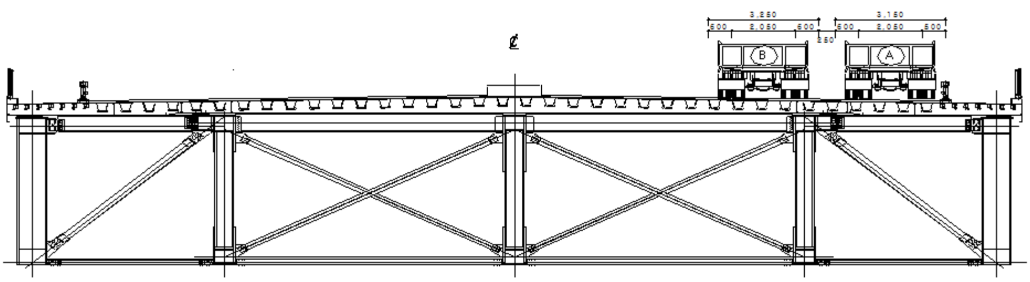

Fig. 5 Load case (LC 3) of static test

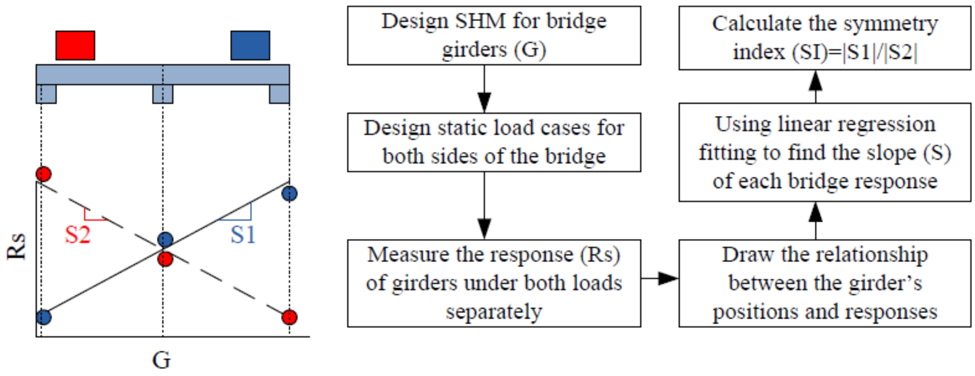

Fig. 6 Flowchart of SI determination

Table 4 Dynamic loads scenarios

Load case	Direction	Lane	Speed	Trucks
LC 1	A2 → A1	2	20 km/h	A
LC 2	A2 → A1	2	30 km/h	B
LC 3	A2 → A1	2	40 km/h	A
LC 4	A2 → A1	2	50 km/h	B
LC 5	A2 → A1	2	60 km/h	A

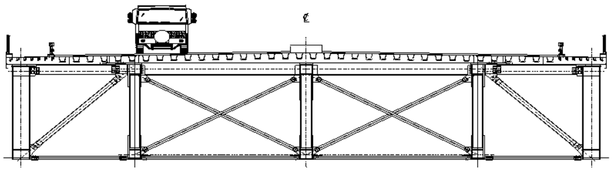

Fig. 7 Truck position for dynamic tests

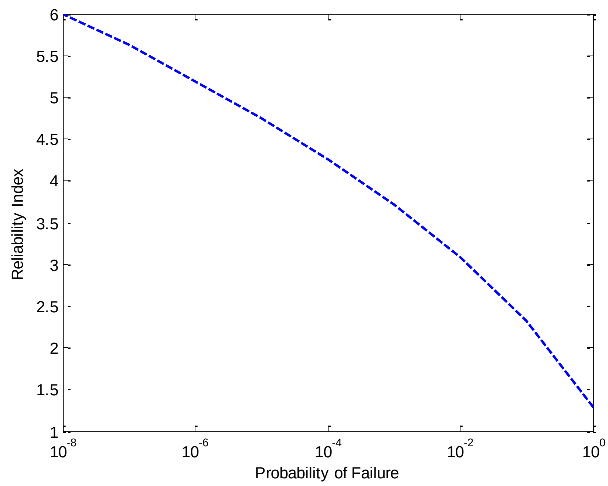

Fig. 8 Reliability index and probability of failure

where R_d and R_s are the dynamic and semi-static responses (i.e., strain and displacement measurements) of bridge girders, respectively. Here, DF is used to assess the load capacity of bridge and examine the safety the bridge girder by comparing it by the design DF value (0.094).

In addition, dynamic torsion of bridge cross section is calculated using displacement measurement. The dynamic torsion angle can be calculated as follows

$$\theta = \arcsin\left(\frac{d_1 - d_5}{B}\right)\frac{180}{\pi} \tag{3}$$

where d_1 and d_5 are the measurement displacement at girders G1 and G5; and B is the distance between the girders.

2.1.2 Reliability analysis

Structural index was estimated to express the bridge reliability, the target reliability index is 3.5 as stated in the AASHTO bridge design specifications (Pablo 2009). Nowak (2012) categorized targeted reliability indices of bridge structures according to the bridge components, the proposed target reliability indices of primary components, which may cause failure or severe damage for other parts of structures, in case failure may occur in single or multiple load path are 3.5 or 5, respectively. While, the targeted reliability for secondary components, which do not influence other structure element in case failure of bridges is 2. Accordingly, the structural reliability index of the bridge girders should be greater than 3.5.

The relationship between the reliability of structure and failure probability is given in Fig. 8 (Nowak 2012). Therefore, the failure probability of structure performance can be also estimated and be used in assessing the reliability of that structure. To assess small failure probability P_f, the subset simulation is developed from the concept of conditional probability and MCMC technique (Papadopoulos *et al*. 2012, Li and Cao 2016). This defines the failure region (F) as the subregion in the x-space that exceeds a response function $g(x)$ below a specific threshold value (b), as follows

$$F = \{x : g(x) < b\} \tag{4}$$

where x is the input random vector which models all uncertain parameters in the system. The target failure probability (P_f) associated with the target failure event may be very small ($P_f \ll 1$). In this case, a numerical solution is required to estimate the failure probability (Li and Cao 2016). Thus, the subset simulation is used to convert a small probability into a product of a sequence of large conditional probabilities, which requires intermediate events to define the failure probability (Li and Cao 2016). Then, the target failure probability of all intermediate events can be calculated as follows

$$P_F = P(F) = P(F_1)\prod_{j=1}^{m-1} P(F_j|F_{j-1}) \tag{5}$$

where $P(F_j|F_{j-1})$ is a setting of the conditional probabilities to achieve the boundary condition (b_j) and further intermediate events (Li and Cao 2016). The simulation of a rare event F is subdivided to the simulations of series of frequently conditional events $F_j|F_{j-1}$. This can be generated successfully using MCMC (Li and Cao 2016). The MCMC can be employed to obtain the required conditional samples $\{x_i\}$ and then the estimator for $\mathrm{P}(F_j|F_{j-1})$

$$P_j = P(F_j|F_{j-1}) \approx \frac{1}{N}\sum_{i=1}^{N} I_{F_j}(g(x_i)) \tag{6}$$

where N is the number of samples in the first simulation level; $I_{F_j}(\cdot)$ is indirect function. After that the MCMC is used to generate conditional samples by starting with an arbitrary sample x_0. The Markov Chain is generated using a transition kernel; therefore, the current state x_i can be transition to the next state x_{i+1}. More details about this method can be found in Wellalage *et al.* (2014) and Li and Cao (2016).

In current study, the failure probability is calculated using the algorithm presented in Li and Cao (2016). The deflection measurements (x_i) are used to calculate the reliability index of the bridge. The allowable deflection of steel bridge (bridge span/800) is used as a target failure region or threshold value (b), and the standard deviation of the deflection is used as conditional probability. Therefore, the limit state function is used here to simulate the failure probability as follows

$$h(x) = b - \frac{1}{n}\sum_{i=1}^{n} x_i \tag{7}$$

Then, the failure probability can be given as

$$P_F = P(h(x) < 0) = \emptyset(-b) \tag{8}$$

where $\emptyset(\cdot)$ is the Cumulative Distribution Function (CDF) of standard normal distribution of the simulation samples of the bridge deflection response.

2.1.3 Mode shapes and damping identification

The FDD has been extensively used for modal identification of different kind of bridges (Magalhães *et al*. 2009, Kim *et al*. 2010, Li *et al*. 2018). This method is used to identify the natural frequency, damping and mode shapes of structures from measurement only (Chen *et al.* 2017). The FDD technique details can be found in Brincker *et al*. (2000, 2001b); it can be briefly summarized as follows: The first step is to obtain the Power Spectrum Density (PSD) matrix of bridge response, $S_{yy}(jw)$. The output is then decomposed at discrete frequencies $w = w_i$ by using the singular value decomposition

$$S_{yy}(jw_i) = U_i G_i U_i^H \tag{9}$$

where U is a matrix of the singular vectors, and G is the diagonal matrix of the scalar singular values. Close to a peak corresponding to the k^{th} mode in the spectrum, only a possible close mode is dominant, and the PSD matrix approximates to a rank-one matrix is decomposed as

$$S_{yy}(jw_i) = U_{i1} G_{i1} U_{i1}^H w_i \rightarrow w_k \tag{10}$$

Therefore, the corresponding first singular value is the auto-spectral density function of a Single Degree Of Freedom (SDOF) system, and the first singular value is an estimate of the mode shapes. From the density function obtained around the peak of the PSD, the dynamic characteristic can be obtained (Chen *et al*. 2017).

The acceleration measurements are also used to estimate the mode shapes. In this study, the strain measurement is transformed into acceleration measurements using regression model identification. The extracted acceleration response is used to estimate the bridge mode shapes. Furthermore, the cross-correlation is used to calculate the bridge damping (Cheynet 2019).

Table 5 Maximum strains (μS) and deflections (mm) recorded during static tests

Section	Sensor	LC1	LC2	LC3	LC4	LC5	LC6
A-A	S5	19.20	13.97	33.98	1.30	-2.02	-3.68
	S9	-3.21	2.05	-6.00	21.88	-25.06	43.38
	S13	-16.38	28.83	45.32	-1.73	3.20	5.65
	D1	-0.28	-0.36	-0.49	-1.92	-1.43	-3.22
	D5	-1.73	-1.29	-3.04	-0.11	-0.28	-0.37
B-B	S19	-1.05	-0.57	-2.13	3.52	4.94	14.03
	S21	4.85	5.24	11.05	2.83	-2.64	2.26
C-C	S25	2.40	0.78	3.16	-12.64	-9.51	-21.27
	S26	-2.68	1.12	-3.27	8.13	16.98	24.90
	S34	-15.15	-11.60	-27.36	2.37	1.91	1.99

3. Results and discussion

3.1 Static dynamic responses

In static test, the low-pass filter is used to extract maximum strains and deflections obtained along the truss girders. The positive and negative strain values produce the tensile and compressive stresses, respectively. Table 5 and Fig. 9 illustrate maximum strains and deflections of recording data. Fig. 9 presents the measurements of strains of S1~S5 and D1~D5 for the LC1, LC3, LC4 and LC 6.

From Table 5, Fig. 9 and statistical analysis of recorded

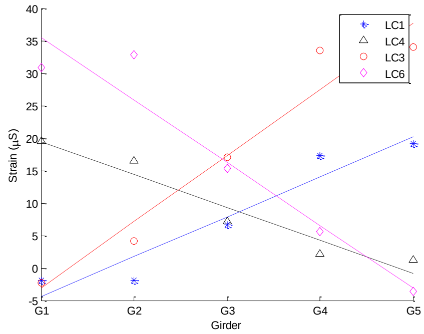

(a)

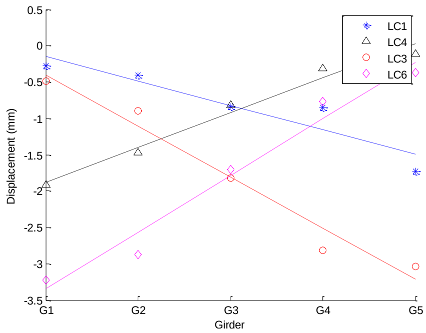

(b)

Fig. 9 Static (a) strains and (b) deflections of bridge girders

data, it can be seen that the maximum strain and deflection are occurred in the cases LC3 and LC6. This is because of the trucks loads effects. The maximum and minimum tensile strains of sensors S1~S5 are 33.98 μS (at S5 with LC3) and 2.17 μS (at S4 with LC4), respectively. Whereas the maximum (-3.68 μS) and minimum (-1.93 μS) compressive strains are observed at S5, with LC6, and S2, with LC1, respectively. Furthermore, compressive strains is observed at sensor S6 (upper chord) during all load cases, from -1.43 μS, with LC2 to -12.56 μS, with LC6; while the opposite side sensor performance is in between tensile (2.79 μS) and compressive (-13.51 μS) strains. Therefore, the compressive strain is mostly occurred in the upper chord members of section A-A; but some un-similarity of the bridge behavior is observed.

In addition, the performance of lower chord is shown in between compresion and tension behaviors; the maximum tensile strains is observed at S8 (23.87 μS with LC6), S10 (27.98 μS with LC6), S14 (24.77 μS with LC3) and S17 (25.33 μS with LC3), and the maximum compressive strain is measured at S17 with LC6 (-3.51 μS). The observations of diagonal chord strains of section A-A show that the range of compressive and tensile strains are high. The maximum compressive and tensile strains measurements of S9 are -25.06 μS and 43.38 μS, respectively; the same is observed at S13, the maximum compressive and tensile strains measurements are -16.38 μS and 45.32 μS, respectively. These results indicate that the fatigue of diagonal chord is higher than other members. In addition, the measurements strain implies that the similarity behavior of bridge cross section is high.

The strain measurements at section B-B show that stress on these members changes between compression and

Table 6 SI of cross section A-A

Case of load	Strain		Displacement	
	Slope	SI	Slope	SI
1	6.15	1.21	-0.33	0.70
4	-5.07		0.48	
2	3.70	0.93	-0.27	0.86
5	-4.00		0.32	
3	10.18	1.06	-0.70	0.90
6	-9.63		0.78	

tension. The maximum range in strains is observed at S19; maximum tensile and compressive strains are 14.03 μS, with LC6, and -2.13 μS, with LC3, respectively. whereas the maximum mean of strains is observed at S21. Furthermore, the performance of strains measurements at section C-C shows that the maximum tensile and compressive strains of upper chord members are 7.16 μS (at S23 with LC6) and -6.12 μS (at S32 with LC3), respectively. In addition, the maximum tensile and compressive strains of lower chord members are 3.16 μS (at S25 with LC3) and -27.36 μS (at S34 with LC3), respectively. Furthermore, the maximum strain range (29.73 μS) is observed at G5 (S34) under all cases of loads. These measurements reveal that the significant strain in the lower chord is compressive strain. Moreover, the observed maximum tensile and compressive strains of diagonal member of section C-C are 24.90 μS, at S26 and -5.23 μS, at S28, respectively. These results indicate that the strain values at the three sections are significantly small.

On the other hand, the maximum deflection is 3.22 mm under two trucks case LC6 is recorded at D1 or G1. In addition, the maximum mean and range of deflection due to all load cases are 1.28 and 2.94 mm. This indicates that the deflection of bridge is small (<< L/800) under static loads effects.

Although, obviously, non-symmetric behavior of bridges can lead to damage (Wang *et al*. 2011), the studies on evaluating the symmerical defromatyion of bridges using only output measurements are very limited. Wang *et al*. (2011) concluded that the displacement measurements under static test can be used in evaluating the symmetrical performance of bridges. Here, a simple novel SI is developed and studied to carry out the same task. Slope of linear fitting is used to estimate the SI, as presented in Eq. (1). Fig. 9 shows the linear fitting of symmetric load cases (LC1 and LC4) and (LC3 and LC6) on the bridge. In addition, the calculation of SI's and fitting slopes are presented in Table 6. The SI is calculated at section A-A for the strains and displacements measurements.

From the data in Table 6, the correlation between SI that calculated by strains and displacements sensors is considerably high. This means that both sensors are very sensitive for the bridge response under affected loads. In addition, the high correlation may result from the linear relationship between performances of strain and displacement sensors under applied loads. Therefore, either of the two measurements can be used to estimate the SI of

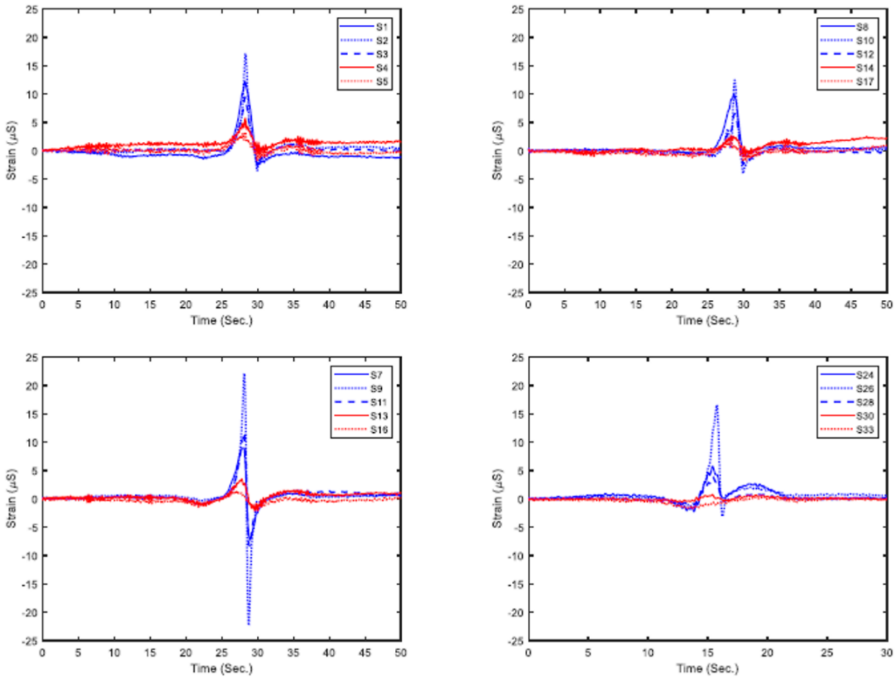

Fig. 10 Strains of bridge under truck speed 60 km/h

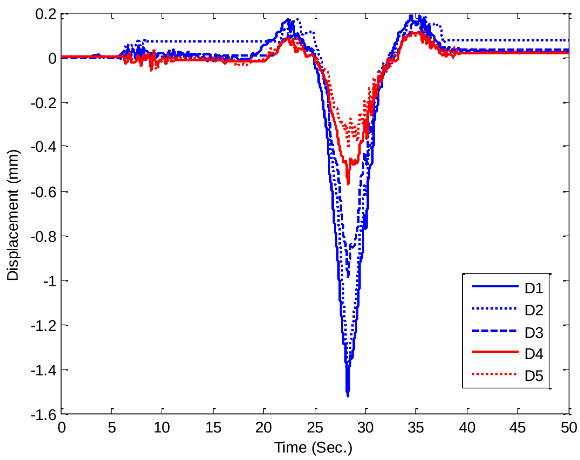

(a)

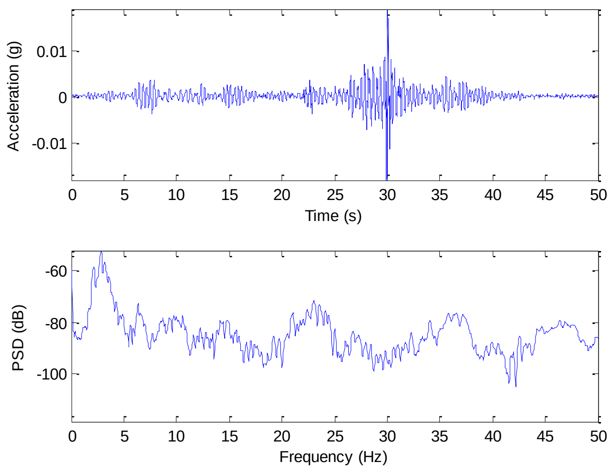

(b)

Fig. 11 (a) Displacements and (b) acceleration (at G2) of bridge under truck speed 60 km/h

the bridge. In addition, from Table 6, it can also be seen that the SI of load cases LC3 and LC6 is close to one. This means that the symmetry behavior of the bridge under double trucks loads is higher than that if it is loaded only with single trucks. Thus, it could be concluded that the bridge behavior under working conditions is mostly symmetry and safe. Herein, it should be mentioned that more numerical and experimental works should be conducted on healthy and unhealthy performances of structures to examine the accuracy of SI calculation.

In the dynamic tests, five velocities of trucks A and B were conducted; here the maximum allowed speed over the bridge is 60 km/h. Therefore, 20~60 km/h speeds were implemented in this test. The range of strains and deflectins are presented in this test; in addition, the dynamic factor is calculated. Figs. 10 and 11 present the filtered strains, displacements and accelerations of bridge performance under truck speed 60 km/h. The maximum responses of the bridgeis observed at G1 and G2; therefore, Table 7 summarize statistical evaluation, range and standard deviation (SD), of the strain's measurements of girder G2 under different traffic speeds.

From Fig. 10, it can be seen that the maximum tensile and compressive strain is occurred at sensor S9, which is located at diagonal member of G2 in section A-A. Similarly, the maximum strains are occurred at sensors S2, S10 and S26; all these sensors are located at G2 in sections A-A and C-C. As also presented in Table 7, it can be seen that the maximum strain range and standard deviation is happened at S9. This reveals that the diagonal members are highly affected by the dynamic loads, similar to what observed in the static tests. In addition, the minimum strain range is observed at section B-B, it means that the expansion joint behavior is safe. Furthermore, the change of range and standard deviation of strains are seen insignificant at

Table 7 Girders G2 strain's responses under different trucks speed (unit: μS)

Speed (km/h)		S2	S9	S10	S19	S26	S27
20	Range	22.39	48.47	19.37	7.05	20.28	9.41
	SD	3.02	5.10	2.38	0.91	2.48	1.90
30	Range	21.16	45.49	18.78	7.73	19.82	8.80
	SD	2.69	4.45	2.13	0.91	2.21	1.67
40	Range	23.58	49.76	19.30	7.38	21.59	9.40
	SD	2.64	4.16	2.04	1.22	1.98	1.64
50	Range	24.37	44.78	19.11	9.84	19.84	9.67
	SD	2.37	3.60	2.23	1.95	2.44	1.74
60	Range	23.23	46.59	19.10	6.78	19.20	9.48
	SD	2.03	3.23	1.54	0.69	2.19	1.74

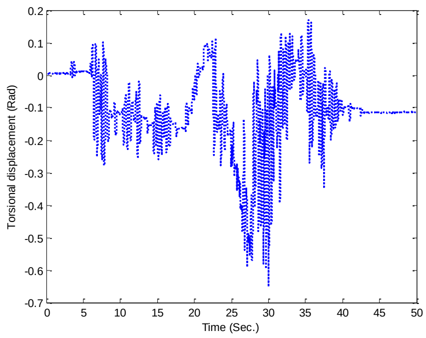

Fig. 12 Mid-span torsion of bridge girder under truck speed 60 km/h

Table 8 Dynamic factor of truss members

Sensor	20 km/h	30 km/h	40 km/h	50 km/h	60 km/h
S2	0.009	0.062	0.037	0.002	0.049
S9	0.028	0.048	0.059	0.026	0.080
S10	0.024	0.038	0.061	0.018	0.077
S19	0.055	0.026	0.048	0.024	0.049
S27	0.082	0.010	0.023	0.049	0.055
S28	0.053	0.030	0.070	0.057	0.003
D1	0.021	0.021	0.079	0.028	0.039
D2	0.014	0.037	0.081	0.014	0.007
D3	0.011	0.011	0.084	0.011	0.040
D4	0.023	0.021	0.056	0.083	0.070
D5	0.083	0.031	0.041	0.056	0.049
Design			0.094		

different trucks speeds. This also reveals that the bridge performance is safe under dynamic loads moving with the speed allowed on the bridge.

Furthermore, the maximum displacement is observed at girders G1 and G2 (1.52 mm and 1.44 mm, respectively). Whereas, the displacement of girders G3, G4 and G5 are 0.99 mm, 0.57 mm and 0.41 mm, respectively. This means

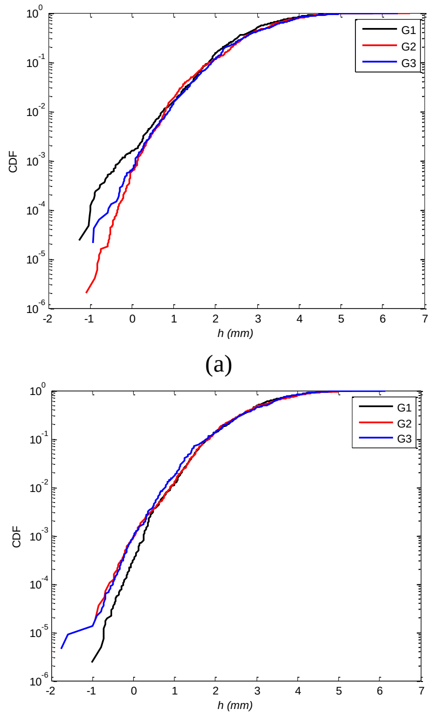

(a)

(b)

Fig. 13 CDF of bridge deflection under truck speeds (a) 20 km/h and (b) 60 km/h

that the dynamic torsion has an effect on the bridge cross section. Fig. 12 presents the torsion of bridge cross section at speed 60 km/h. The torsion is affected the girder while the truck passes, this means the bridge sees torsion during the traffic loads. Caring out the torsion calculations at different truck speeds, it can be seen that the maximum twisting angle observed at all the tested bridge sections are 0.39, 0.44, 0.40, 0.52, 0.65 radian at 20 km/h, 30 km/h, 40 km/h, 50 km/h and 60 km/h. Therefore, the torsion-induced twisting angles under moving trucksare small and insignificant compared with the limits stated in the AASHTO.

Additionally, it is important to examine the dynamic characteristics of the bridge, in particular the dominant natural frequencies. The deviation between the current measured and the design frequency of the bridge could reveal the deterioration that occurred during the service period. Fig. 11(b) shows the calculation frequency under truck speed 60 km/h. The bridge frequency was calculated using acceleration measurements and Welch's method. The dominant frequency of the bridge under 20 km/h, 30 km/h, 40 km/h, 50 km/h and 60 km/h are 3.03, 2.97, 2.97, 2.97 and 2.83 Hz, respectively. The dominant frequency that extracted at G1 is equal that extracted at G2. The design value of bridge frequency is 2.48 Hz. This indicates that the dynamic behavior of the bridge is safe.

Meanwhile, the DF of bridge girders is calculated and presented in Table 8. The maximum dynamic effects that extracted from strain measurements are observed at S9 (0.080) and S27 (0.084) with truck speed 60 km/h and 20 km/h, respectively. Furthermore, the maximum DF, that calculated by displacement measurements, is observed with

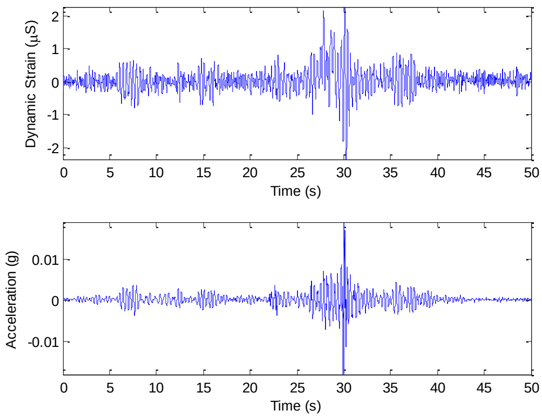

(a)

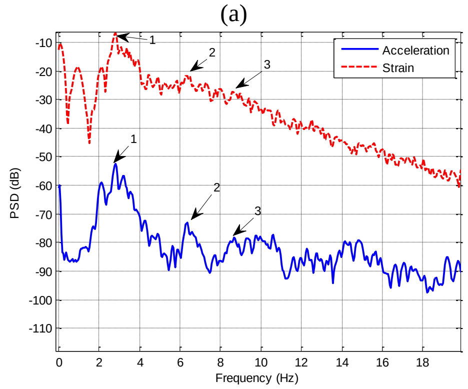

(b)

Fig. 14 Acceleration and extracted dynamic strain of (a) signals and (b) frequency modes

truck speed 40 km/h at girders G1, G2 and G3, while that was observed at G4 and G5 under trucks speeds 50 km/h and 20 km/h. This indicates that the low speed of trucks influences dynamic behaviors on the bridge girders more than high speeds. On the other hand, the maximum DF is lower than the design value (0.094), it means that the dynamic behavior of the bridge is safe and under the design limits.

3.2 Bridge reliability

The maximum deflection under the travel of trucks over the bridge is observed at girders G1~G3; whereas the deflection can be negligible at girders G4 and G5. Therefore, the reliability index is calculated at girders G1 to G3. Herein, the probability of failure is calculated relative to the allowable AASHTO deflection of bridge girders, span/800. Here, the Eqs. (7) and (8) are used to estimate the failure probability and CDF of the bridge response. The failure probability of the bridge is zero if we calculated it using the allowable value of the limit state; therefore, the reliability index of the bridge is higher than 3.50 (see Fig. 8). This indicates that the bridge reliability is safe. For more safety, we have studied the reliability of dynamic bridge deflection relative to maximum static deflection (3.22 mm). Fig. 13 shows the CDF of the girder's responses under truck speeds 20 and 60 km/h. From Fig. 13, it can be seen that more that 95% of the dynamic bridge deflection is less than the maximum static deflection. In addition, the calculation

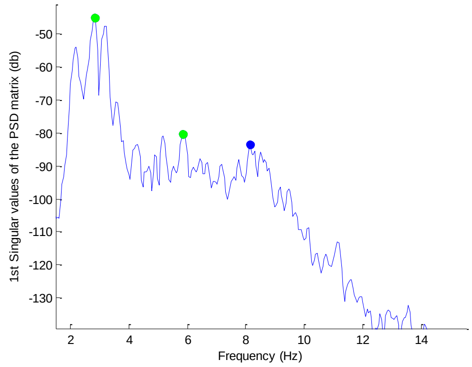

(a)

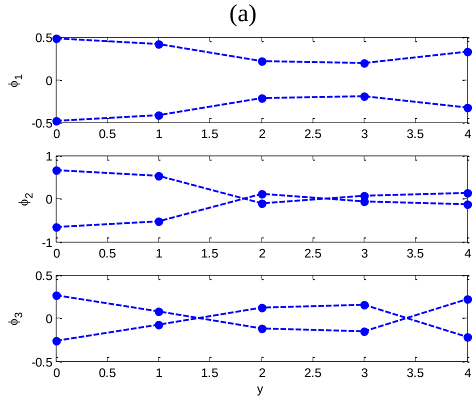

(b)

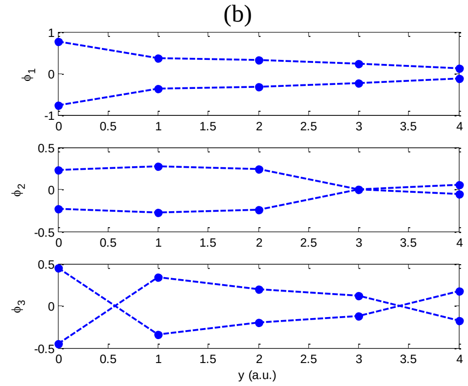

(c)

Fig. 15 Singular values of bridge response under truck speed 60 km/h, and the identification modal shapes of the bridge under truck speeds (b) 20 km/h and (c) 60 km/h

failure probabilities of girders G1, G2 and G3 are 1.5×10^{-3}, 5.9×10^{-4} and 6.6×10^{-4}, respectively, for the bridge response under 20 km/h. Also, the G1, G2 and G3 failure probabilities of the bridge deflection under 60 km/h are 3.2×10^{-4}, 9.1×10^{-4} and 9.2×10^{-4}, respectively. These results reveal that the failure probability of the bridge is affected by the truck positions. In addition, the low speed is more effective than high speed on the probability of bridge failure. This should be occurred due to the load time effects on the bridge. Furthermore, the estimated reliability index, from Fig. 8 by linear fitting, is greater than 3.10 for the girder G1 under 20 km/h and over than 3.50 for the other performances of the girders. This means that the bridge reliability is still in safe zone with our consider, so the probability of bridge failure is small.

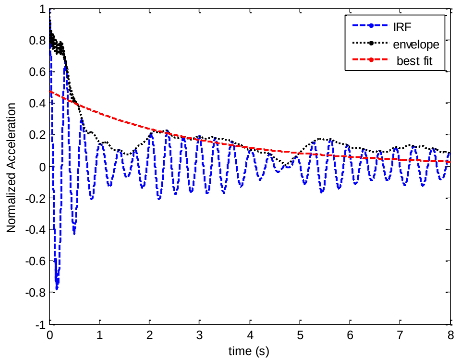

(a)

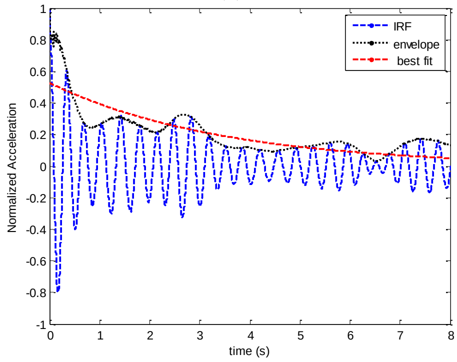

(b)

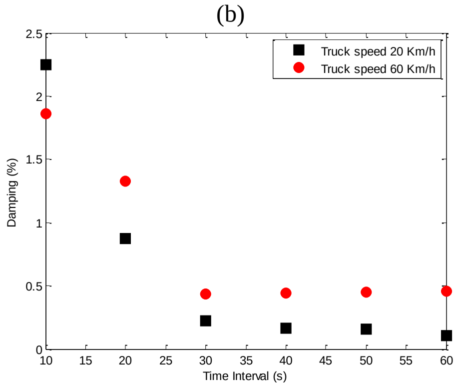

(c)

Fig. 16 The IRF of bridge girder under (a) 20 km/h; (b) 60 km/h; (c) the damping ratios with different time intervals

3.3 Mode shapes and damping

To study the mode shape of bridge cross section, the strain sensors S1~S5 are used. The dynamic strain of bridge response under 20 and 60 km/h are used. The dynamic strain is the results of strain measurements after removing the filtered signals. It is known that the acceleration uses to extract the more shapes of structures. So, first the dynamic strain is evaluated. Dynamic strain, acceleration signals and movements modes of the bridge response under 60 km/h at G2 are presented in Fig. 14.

From Fig. 14, it can be seen that the peaks of dynamic behaviors of dynamic strain are correlated with that observed by acceleration measurements. The maximum dynamic strain and acceleration is observed at the same time (time 30 sec). In addition, the three models of the bridge frequency, as presented in Fig. 14(b), of the bridge by dynamic strain are 2.83, 6.30, 8.60 Hz, and that by acceleration are 2.83, 6.35, 8.69 Hz. These results indicate that the dynamic strain can be used to extract the mode shapes of the bridge.

The FDD is used to estimate the three mode shapes of the bridge cross section under trucks speed 20 and 60 km/h. The FDD that designed by Cheynet (2019) is utilized in this study to estimate identification modal shapes and damping of the bridge. The PSD of singular value for the dynamic strain of the bridge cross section is extracted using FDD. Fig. 15 shows the singular values of dynamic strain of bridge response under 60 km/h and modes shapes of the bridge. The maximum peaks of singular values are selected to calculate mode shapes of the bridge.

Furthermore, from Figs. 15(b) and (c), it can be seen that the bending mode shape is the first mode, whereas the second and third modes are torsion shape. The dominant frequency is the first mode, and the modal frequency of it under 20 and 60 km/h are 3.03 and 2.83 Hz, respectively. The second modal frequency of the bridge under 20 and 60 km/h is 6.00 and 5.86 Hz, respectively; whereas the modal frequency of the third mode is 8.20 and 8.15 Hz for the speeds 20 and 60 km/h, respectively. The maximum changes in the modal shapes are observed at bending modal shape; whereas the torsion modal shapes are almost same. These results indicate the significant bridge behavior is occurred due to bending stress, and torsion effective is small under changes of speeds.

Meanwhile, the bridge Impulse Response Function (IRF) of the bridge performance is calculated using unbiased cross-covariance function of the acceleration measurements of girder G2 (Cheynet 2019). The Helbert transformation (Kaloop *et al*. 2016) is used to estimate the envelope of the IRF, and the exponential model in Matlab is used to estimate the best fitting of the envelope curve and calculate the damping of the bridge response. Different time interval is used to assess the behavior of bridge under different trucks speeds. Fig. 16 presents the damping calculation for the bridge responses under 20 and 60 km/h of 10 second interval. Fig. 16(c) shows the estimated results of damping ratios with different time intervals; it can be seen that the damping ratio has a tendency toward stabilization when the time interval is greater than 30 s. Therefore, we deduce that the time interval of IRF should last at least 30 s. The corresponding damping ratio of bridge response at 30 s time interval is 0.226 and 0.438% under truck speed 20 and 60 km/h. this indicates that the bridge damping is doubled when the truck speed increased by 40 km/h; in addition, the damping of the bridge is within the steel bridges limit state based on AASHTO standards.

4. Conclusions

This contribution presents a novel behavior assessment of bridges for vibration based nondestructive test of short period structural health monitoring systems. Strain, displacement and acceleration measurements for Sungsu bridge are adapted and applied as a metric for fault diagnosis of the bridge. Symmetry index is conducted using static behavior test of the bridge. In addition, the bridge dynamic factor, frequency modes and reliability are assessed using dynamic tests. The FDD and MCMC are applied to estimate the frequency models and reliability, respectively, and the following conclusions are obtained:

The measurements of NDT-short period SHM can be used as indicator to assess the performance of bridges in static and dynamic behaviors. In addition, the novel SI is a simple index can be used to evaluate the behavior of bridges under static loads. In our case, the symmetry behavior of the bridge under double trucks loads is higher than that if it is loaded by single trucks. This reveals that the bridge behavior under working case is symmetric and safe. Herein, it should be mentioned that more numerical and experimental works should be conducted on healthy and unhealthy performances of structures to examine the accuracy of SI calculation.

Dynamic strain can be used to evaluate the dynamic behavior of bridges. It is found a correlated with the acceleration measurements. Therefore, it can be used to estimate the mode shapes and damping of bridges using FDD method. in our case, the results indicate that a significant of Sungsu bridge behavior is occurred due to bending stress, and torsion effective is small under changes of speeds, and the bridge damping is doubled when the truck speed increased; in addition, the dynamic behavior of the bridge is within the steel bridges limit state based on AASHTO standards.

The results of the reliability analysis of the bridge reveal that the failure probability of the bridge is affected by the truck positions. In addition, the low speed is higher affective than high speed on the probability of bridge failure. Furthermore, the estimated reliability index indicates that the bridge reliability is still in safe zone with our consider, so the probability of bridge failure is small.

Conflict of interest

The authors declare that there is no conflict of interests regarding the publication of this paper.

Acknowledgments

This work was supported by Post-Doctor Research Program in 2019 through the Incheon National University (INU), Incheon, South Korea.

References

Abbas, M. and Mahmood, S. (2018), “Structural health monitoring (SHM) and determination of surface defects in large metallic structures using ultrasonic guided waves”, *Sensors*, **18**(11), e3958. https://doi.org/10.3390/s18113958.

Akköse, M., Hugo, C. and Maria, Q. (2017), “Modal response identification of a highway bridge under traffic loads using frequency domain decomposition (FDD)”, *Chall. J. Struct. Mech.*, **3**(2), 63-71. https://doi.org/10.20528/cjsmec.2017.03.009.

Barker, M., Imhoff, C., McDaniel, W.T. and Frederick, T.L. (1999), “Field testing and load rating procedures for steel girder bridges”, Report-RDT 99-004, University of Missouri, Columbia, USA.

Beck, J.L. and Au, S. (2002), “Bayesian updating of structural models and reliability using Markov chain Monte Carlo simulation”, *J. Eng. Mech.*, **128**(4), 380-391. https://doi.org/10.1061/(asce)0733-9399(2002)128:4(380).

Brincker, R., Zhang, L. and Andersen, P. (2000), “Modal identification from ambient responses using frequency domain decomposition”, *Proceedings of the Imac-Xviii: A Conference on Structural Dynamics*, San Antonio, Texas, USA, February.

Brincker, R., Palle, A. and Cantieni, R. (2001a), “Identification and level 1 damage detection of the Z24 highway bridge by frequency domain decomposition”, *Exp. Tech.*, **25**(6), 51-57. https://doi.org/10.1111/j.1747-1567.2001.tb00047.x.

Brincker, R., Zhang, L. and Andersen, P. (2001b), “Modal identification of output-only systems using frequency domain decomposition”, *Smart Mater. Struct.*, **10**(3), 441-445. https://doi.org/10.1088/0964-1726/10/3/303.

Chang, S., Yee, J. and Lee, J. (2009), “Necessity of the bridge health monitoring system to mitigate natural and man-made disasters”, *Struct. Infrastruct. Eng.*, **5**(3), 173-197. https://doi.org/10.1080/15732470601130378.

Chen, Z., Zhou, X., Wang, X., Dong, L. and Qian, Y. (2017), “Deployment of a smart structural health monitoring system for long-span arch bridges: A review and a case study”, *Sensors*, **17**, 2151. https://doi.org/10.3390/s17092151.

Cheynet, E. (2019), “Modal parameters identification from ambient vibrations”, MATLAB Central File Exchange. www.mathworks.com.

Commander, B., Grimson, J., Varela-Ortiz, W., Stanton, T., Lugo, C. and Hansler, G. (2008), “Field testing and load rating report, bridge S-1090, camp casey, South Korea”, Report US Army Crops of Engineers, Engineering Research and Development Center, USA.

Decò, A. and Frangopol, D. (2011), “Risk assessment of highway bridges under multiple hazards”, *J. Risk Res.*, **14**(9), 1057-1089. https://doi.org/10.1080/13669877.2011.571789.

Hu, W., Cunha, A., Caetano, E., Magalhães, F. and Moutinho, C. (2010), “LabVIEW toolkits for output-only modal identification and long-term dynamic structural monitoring”, *Struct. Infrastruct. Engineering*. **6**(5), 557-574. https://doi.org/10.1080/15732470903068672.

Jeong, Y., Kim, W., Lee, I. and Lee, J. (2018), “Bridge inspection practices and bridge management programs in China, Japan, Korea and U.S.”, *J. Struct. Integr. Maint.*, **3**(2), 126-135. https://doi.org/10.1080/24705314.2018.1461548.

Pablo, R.M. (2009), “Risk assessment of highway bridges: A reliability-based approach”, *Proceedings of the 2008 IAJC-IJME International Conference, Paper 158, ENT 209 Risk*, Nashville, USA, November.

Kaloop, M.R. and J.W. Hu. (2016), “Dynamic performance analysis of the towers of a long-span bridge based on GPS monitoring technique”, *J. Sens.*, **2016**, 7494817. https://doi.org/10.1155/2016/7494817.

Kaloop, M.R., Hu, J.W. and Sayed, M.A. (2016), “Yonjung high-speed railway bridge assessment using output-only structural health monitoring measurements under train speed changing”, *J. Sens.*, **2016**, 4869638. https://doi.org/10.1155/2016/4869638.

Kaloop, M.R., Hwang, W.S., Elbeltagi, E., Beshr, A. and Hu, J.H. (2019), “Evaluation of Dorim-Goh bridge using ambient trucks through short-period structural health monitoring system”, *Struct. Eng. Mech., Int, J.*, **69**(3), 347-359. https://doi.org/10.12989/sem.2019.69.3.347.

Kim, B., Lee, J. and Lee, D. (2010), “Extracting modal parameters of high-speed railway bridge using the TDD technique”, *Mech. Syst. Signal Process.*, **24**(3), 707-720.

https://doi.org/10.1016/j.ymssp.2009.11.010.

Kim, J., Sim, S., Cho, S., Yun, C. and Min, J. (2016), "Recent R & D activities on structural health monitoring in Korea", *Struct. Monit. Maint.*, **3**(1), 91-114.

Koh, H., Lee, H., Kim, S. and Choo, J. (2009), "Monitoring of bridges in Korea", *Struct. Health Monit.*, **2009**, 1-23.

Li, H. and Cao, Z. (2016), "Matlab codes of subset simulation for reliability analysis and structural optimization", *Struct. Multidiscipl. Optim.*, **54**(2), 391-410. https://doi.org/10.1007/s00158-016-1414-5.

Li, Z., Feng, M., Luo, L., Feng, D. and Xu, X. (2018), "Statistical analysis of modal parameters of a suspension bridge based on Bayesian spectral density approach and SHM data", *Mech. Syst. Signal Process.*, **98**, 352-367. https://doi.org/10.1016/j.ymssp.2017.05.005.

Magalhães, F., Cunha, A. and Caetano, E. (2009), "Online automatic identification of the modal parameters of a long span arch bridge", *Mech. Syst. Signal Process.*, **23**(2), 316-329. https://doi.org/10.1016/j.ymssp.2008.05.003.

Mccarthy, L. (2012), "Probabilistic analysis of indeterminate highway bridges considering material nonlinearity probabilistic analysis of indeterminate highway bridges", MS.c. Dissertation, Dublin Institute of Technology, Dublin, Ireland.

Nowak, A. (2012), "Risk analysis and target reliability for bridges", MID-AMERICA, Transportation Center, USA.

Papadopoulos, V., Giovanis, D., Lagaros, N. and Papadrakakis, M. (2012), "Accelerated subset simulation with neural networks for reliability analysis", *Comput. Methods Appl. Mech. Eng.*, **223-224**, 70-80. https://doi.org/10.1016/j.cma.2012.02.013.

Peiris, A. and Harik, I. (2016), "Load testing of bridges for load rating", *Proceedings of the 7th International Conference on Sustainable Built Environment, ICSBE2016-116*, Kandy, Sri Lanka, December.

Proppe, C. (2017), "Markov chain Monte Carlo simulation methods for structural reliability analysis", *Procedia Eng.*, **199**, 1122-1127. https://doi.org/10.1016/j.proeng.2017.09.226.

Seo, J., Phares, B., Lu, P., Wipf, T. and Dahlberg, J. (2013), "Bridge rating protocol using ambient trucks through structural health monitoring system", *Eng. Struct.*, **46**, 569-580. https://doi.org/10.1016/j.engstruct.2012.08.012.

Sgambi, L., Garavaglia, E., Basso, N. and Bontempi, F. (2014), "Monte Carlo simulation for seismic analysis of a long span suspension bridge", *Eng. Struct.*, **78**, 100-111. https://doi.org/10.1016/j.engstruct.2014.08.051.

Song, X., Ma, H. and Wang, K. (2017), "A new developed modal parameter identification method based on empirical mode decomposition and natural excitation technique", *Procedia Eng.*, **199**, 1020-1025. https://doi.org/10.1016/j.proeng.2017.09.270.

Wang, Y., Liu, X. and Fang, C. (2011), "Damage detection of bridges by using displacement data of two symmetrical points", *J. Perform. Constr. Facil.* **26**(3), 300-311. https://doi.org/10.1061/(asce)cf.1943-5509.0000240.

Wellalage, N.K., Zhang, T. and Dwight, R. (2014), "Calibrating Markov chain–based deterioration models for predicting future conditions of railway bridge elements", *J. Bridge Eng.*, **20**(2), 04014060. https://doi.org/10.1061/(asce)be.1943-5592.0000640.

Xiao, F. (2016), "Structural health monitoring and bridge condition assessment", Ph.D. Dissertation, College of Engineering and Marine, University of Alaska Fairbanks, AK, USA.

Yanweerasak, T., Pansuk, W., Akiyama, M. and Frangopol, D. (2018), "Life-cycle reliability assessment of reinforced concrete bridges under multiple hazards", *Struct. Infrastruct. Eng.*, **14**(7), 1011-1024. https://doi.org/10.1080/15732479.2018.1437640.

Yilmaz, T., Banerjee, S. and Johnson, P. (2018), "Uncertainty in risk of highway bridges assessed for integrated seismic and flood hazards", *Struct. Infrastruct. Eng.*, **14**(9), 1182-1196. https://doi.org/10.1080/15732479.2017.1402065.

Zhang, L. and Wang, T. and Tamura, Y. (2005), "A frequency-spatial domain decomposition (FSDD) technique for operational modal analysis", *Proceedings of the 1st International Operational Modal Analysis Conference*, Copenhagen, Denmark, April.

Zolghadri, N. (2017), "Short and long-term structural health monitoring of highway bridges", Ph.D. Dissertation, Utah State University, UT, USA.

HJ